# Multi-layer FFR-aided OFDMA-based Networks using Channel-Aware Schedulers

# Multi-layer FFR-aided OFDMA-based Networks using Channel-Aware Schedulers

Jan García-Morales, *Student Member, IEEE*, Guillem Femenias, *Senior Member, IEEE*, Felip Riera-Palou, *Senior Member, IEEE*, and John S. Thompson, *Fellow, IEEE*

***Abstract*—In OFDMA networks, the use of universal frequency reuse improves overall cell capacity at the cost of very high levels of inter-cell interference (ICI) particularly affecting the users located in the cell-edge regions. In order to provide a better quality of experience to cell-edge users while still achieving high spectral efficiencies, conventional fractional frequency reuse (FFR) schemes split the cells into inner and outer regions (or layers) and allocate disjoint frequency resources to each of these regions by applying higher frequency reuse factors to the outer regions. Recently, multi-layer FFR-aided OFDMA-based designs, splitting the cell into inner, middle and outer layers have been proposed with the aim of further improving the throughput fairness among users. This paper presents an analytical framework allowing the performance evaluation and optimization of multi-layer FFR-aided OFDMA-based networks. Tractable mathematical expressions of the average spectral efficiency are derived and used to pose optimization problems allowing network designers to achieve the optimal trade-off between spectral efficiency and fairness. Analytical and simulation results clearly show that, irrespective of the channel-aware scheduler in use, multi-layer FFR-schemes can outperform the conventional two-layer FFR architectures.**

***Index Terms*—OFDMA cellular networks, multi-layer FFR, channel-aware schedulers, spectral efficiency, optimization.**

## I. Introduction

### A. Motivation

ORTHOGONAL frequency division multiple access (OFDMA) is one of the most prominent air-interfaces in modern cellular standards [1]. Owing to the orthogonality among subcarriers, OFDMA makes the intra-cell interference negligible. However, inter-cell interference (ICI) remains an issue due to the use of *aggressive* high spectral efficiency universal frequency reuse plans where all cells use the same set of frequency subbands (reuse-1). In this setup, ICI critically affects the mobile stations (MSs) located near the cell-edge because the serving base station (BS) and the nearest interfering ones are located at similar distances. Unfortunately, the implementation of less aggressive conventional frequency reuse arragements like, for instance, the well-known reuse-3 scheme, decreases ICI at the cost of sacrificing spectral efficiency. With the aim of mitigating the high levels of ICI experienced by the cell-edge users while still achieving high spectral efficiencies, multiple ICI control (ICIC) strategies have been proposed in the literature (see, for instance, [2] and references therein), among which, *static* fractional frequency reuse (FFR) has been shown to provide a good tradeoff among cell-edge throughput enhancement, provision of high spectral efficiency and implementation complexity [3].

J. García-Morales, G. Femenias and F. Riera-Palou are with the Mobile Communications Group, University of the Balearic Islands, Palma 07122, Illes Balears, Spain (e-mail: {jan.garcia,guillem.femenias,felip.riera}@uib.es).

J. Thompson is with the Institute for Digital Communications, School of Engineering, University of Edinburgh, Edinburgh EH9 3JL, U.K. (e-mail: john.thompson@ed.ac.uk).

The conventional FFR scheme splits the cell into two layers, the inner and the outer ones (also known as cell-center and cell-edge regions). A low frequency reuse factor is used for the inner-cell MSs (typically reuse-1), less affected by co-channel interference, and a larger frequency reuse factor is selected for the outer-cell MSs (e.g., reuse-3), which are more prone to ICI. In spite of their advantages, the conventional two-layer FFR has also some drawbacks. On one hand, when the area covered by the inner layer is large, the MSs located at the edge of this layer already suffer from high levels of ICI. On the other hand, when the area covered by the outer layer expands, the spectrum utilization decreases and the spectral efficiency drops. Therefore, it can be concluded that, in order to provide a certain degree of fairness among users located in different areas of the cell while still achieving high spectral efficiencies, both inner and outer layers should not be too large. In an attempt to reconcile these two conflicting situations, the use of FFR schemes with more than two layers has been recently proposed as a promising ICIC approach for next generation cellular systems (see [4] and references therein). The rationale behind the multi-layer FFR configuration is that by incorporating middle layers in between the inner and outer ones, the fairness among MSs located in different layers can be improved without sacrificing (and even often increasing) the overall cell throughput.

Regardless of the particular ICIC technique in use, spectral efficiency can be further enhanced by using channel-aware schedulers that, within each scheduling period, allocate the radio resources to users with favourable channel conditions (i.e., users experiencing high levels of signal-to-interference-plus-noise ratios (SINR)), thus exploiting multiuser diversity. Maximum SINR (MSINR) schedulers, however, optimize the system spectral efficiency at the cost of sacrificing fairness among MSs. By contrast, the proportional fair (PF) scheduler has been shown to provide a good tradeoff between spectral efficiency and fairness [5]. Then, the use of multi-layer FFR-aided OFDMA-based systems in combination with PF-based channel-aware schedulers seems to be a very interesting approach to deal with the deleterious effects of ICI.

### B. Related work

Analytical performance evaluations of conventional two-layer FFR-aided OFDMA-based cellular networks have been tackled using Poisson Point Processes (PPPs) to model the location of the BSs [6], [7]. These approaches allow characterization of the system performance by spatially averaging over all possible network realizations, but they cannot accurately analyze the performance of a given cell, a metric of particular importance to network designers that, provided a planned set of BS locations along with traffic load conditions, will be interested in calculating the performance obtained within a specific region in the coverage area of the network.

In order to characterize the performance of a specific cell in the network, there are many studies in the literature specifically focusing on the optimization of the inner radius, as well as the inner region bandwidth of the conventional two-layer FFR-based layout [8]–[16]. In particular, Fan Jin *et al.* [8] studied a two-layer FFR-aided twin-tier OFDMA network where stochastic geometry was used to characterize the random distribution of femtocells, and the macrocells were overlaid on top of the femtocells following a regular tessellation. However, the analytical framework was limited to resource allocation schemes based on the round robin (RR) scheduling policy, thus neglecting the gains that can be achieved by using channel-aware PF and MSINR schedulers. Similar approaches, lacking the consideration of scheduling policies and small scale fading, were also proposed by Assaad in [9] and Najjar *et al.* in [10] to optimize the two-layer FFR-based parameters in a single-tier network. These limitations were overcome in part by Xu *et al.* in [11] (see also [12]) and Garcia-Morales *et al.* in [13], but only for opportunistic MSINR schedulers. The impact the selection of frequency reuse factor and distance thresholds has on the performance of conventional two-layer FFR schemes in OFDMA-based dense networks was analyzed in [14]–[16]. However, none of these afore mentioned studies considered the use of multi-layer FFR-aided schemes.

In contrast to the above background work, [4], [17]–[19] consider the use of multi-layer FFR schemes to control the ICI. Xie and Walke in [17] proposed a three-layer FFR scheme using reuse-1 and low transmit power for the inner layer, reuse-3 and moderate transmit power for the middle layer, and reuse-9 and high transmit power for the outer layer. A theoretical analysis of a series of reuse partitioning approaches was carried out in this paper using mathematically tractable expressions, but only considering the pathloss effect and thus precluding any attempt to analyze the system performance with the use of channel-aware schedulers. Ghaffar and Knopp in [18], also proposed a three-layer scheme. In particular, reuse-1 was used for the inner layer and reuse-3/2 for the middle and outer layers. The use of this approach provided a reduction of power consumption at the BSs leading to an improvement of the average spectral efficiency but at the cost of increasing the ICI. A multi-layer soft frequency reuse (SFR) scheme was proposed by Yang in [19] where different power levels were allocated to each layer. This approach can achieve a better interference pattern than that obtained using a two-layer SFR, thus improving the overall spectral efficiency. In [18] and [19], the average cell and per-layer spectral efficiencies were formulated, but the authors did not provide either closed-form solutions or mathematically tractable expressions to deal with these metrics. Thus, only results obtained through Monte-Carlo simulations were presented. Particularly interesting is the work of Wang *et al.* in [4], where a mathematically tractable multi-layer FFR model was proposed. Moreover, optimal designs and closed-form expressions of the average spatial capacities of certain typical regions of a cell were derived. One of the main conclusions of this work was that multi-layer schemes can provide better average spatial capacity and fairness than the traditional two-layer scheme. The main limitation of this work, however, was the use of rather unrealistic assumptions such as neglecting the small scale fading effects and, consequently, limiting the proposed analytical framework to resource allocation schemes based on the RR scheduling policy.

### C. Contributions of the paper

In this paper, a novel analytical framework allowing the analysis and optimization of multi-layer FFR-aided OFDMA-based cellular networks is introduced. Compared to previous studies, our main contributions in this paper can be summarized as follows:

- In order to characterize the wireless channel effects, closed-form analytical expressions for the statistical distribution of the SINR are first derived. These are used to obtain tractable mathematical expressions of the average cell throughput for the benchmark two-layer setup and the proposed four-layer FFR-based configuration.
- Based on the statistical channel characterization and the cell throughput expressions, an analytical framework is provided. This can evaluate the impact any of the FFR layers may produce on the average cell throughput, the average throughput per layer or the average throughput experienced by the *worst* MSs in each layer. These metrics are first derived for the PF scheduler and then simplified for the RR scheduling rule.
- In order to select the size of the FFR-related spatial and spectral partitions, two multi-layer FFR-based optimal designs, namely the area-proportional design (ApD) and the free-design (FrD), are introduced. Furthermore, for both ApD and FrD approaches, an optimization problem is posed which can maximize the max-min throughput fairness among users located in different layers.
- Analytical results, which are corroborated by extensive Monte-Carlo simulations, confirm that, when compared to conventional two-layer designs, multi-layer FFR-aided ODMA-based schemes can serve to improve fairness among MSs without sacrificing overall spectral efficiency.

### D. Paper organization

The rest of the paper is organized as follows. In Section II the cellular network model is presented along with a statistical characterization of the channel under consideration. Section III, assuming the use of a PF channel-aware scheduler, elaborates on the analytical framework used to derive the

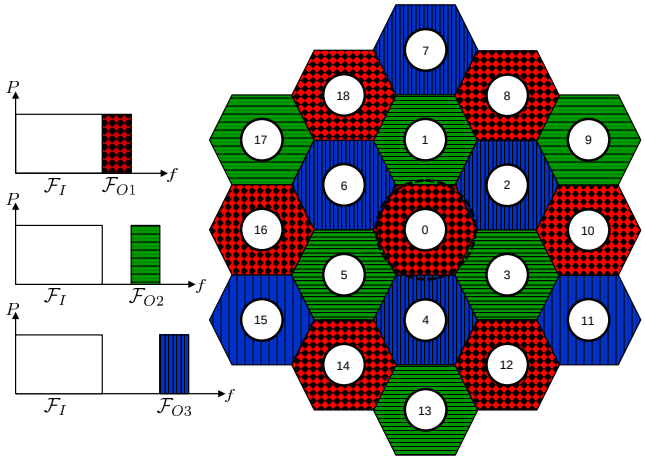


Fig. 1: Schematic representation of the two-layer FFR-aided OFDMA-based cellular network.

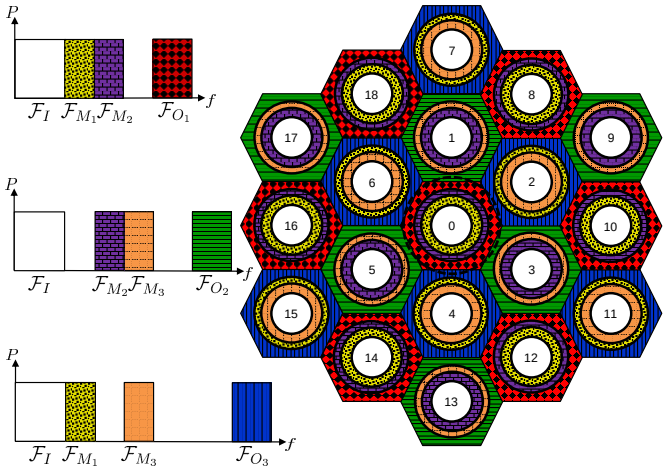


Fig. 2: Schematic representation of a four-layer FFR-aided OFDMA-based cellular network.

average throughput performance provided by a given BS to each of the layers. The special case of the RR scheduling rule is also discused. Optimization set-ups for different multi-layer FFR designs are presented in Section IV. Focusing on each FFR design, extensive analytical and simulation results are provided in Section V. Finally, the main outcomes of this paper are recapped in Section VI.

## II. Cellular network model

Let us consider the downlink of an OFDMA-based cellular system where a set of BSs are assumed to be regularly arranged over the whole coverage area. This cellular environment can be modeled as a regular tessellation of hexagonally-shaped coverage areas, as shown in Figs. 1 and 2, with the BSs located at the centre of the hexagons. For the sake of analytical tractability, the central cell, covering a spatial region $\mathcal{H}$ and served by BS 0, which will be referred to as the tagged BS, will be approximated by a circle whose area is the same as the hexagonal one. That is, assuming that the side of the regular hexagon is $R_h$, the radius of the circular cell is $R = R_h\sqrt{3\sqrt{3}/(2\pi)}$, and the total cell coverage area is $A_r^{\mathcal{H}} = \pi(R^2 - R_0^2)$, where $R_0$ is the minimum distance of a MS from its serving BS.

The locations of the MSs at a given time instant are assumed to form a stationary PPP of normalized intensity $\lambda$ (measured in MSs per unit area). A consequence of this assumption is that the probability distribution of the number of MSs $M_{\mathcal{S}}$ falling within any spatial region $\mathcal{S}$ of area $A_r^{\mathcal{S}}$ follows a Poisson distribution, thus implying

$$\Pr\{M_{\mathcal{S}} = k\} = \frac{(\lambda A_r^{\mathcal{S}})^k e^{-\lambda A_r^{\mathcal{S}}}}{k!}. \quad (1)$$

### A. Two-layer FFR network layout

In order to control the ICI, MSs in a two-layer FFR network are classified according to the received average SINR as either inner-cell MSs, when the received average SINR is above a given threshold. Otherwise, they are classified as outer-cell MSs. Moreover, non-overlapping resources (subcarriers) are allocated to inner-cell and outer-cell MSs, while employing a frequency reuse factor equal to one (reuse-1) for the inner-cell MSs and a higher frequency reuse factor for the outer-cell MSs that is assumed to be 3 in this paper (reuse-3). For the sake of analytical tractability, inner and outer regions (or layers) will be separated by a circumference of radius $R_{th}$ (threshold distance).

The total system bandwidth is exploited by means of a set $\mathcal{F}_T$ of $N_T$ orthogonal subcarriers with a sufficiently small bandwidth $\Delta f$ such that all subcarriers experience frequency flat fading. The set $\mathcal{F}_T$ is split into a set $\mathcal{F}_I$ of subcarriers allocated to the inner layer and a set $\mathcal{F}_O = \mathcal{F}_T \backslash \mathcal{F}_I$ of subcarriers allocated to outer layers. The set $\mathcal{F}_O$ is further split into three equal parts, namely $\mathcal{F}_{O1}$, $\mathcal{F}_{O2}$ and $\mathcal{F}_{O3}$, which are allocated to outer-cell MSs in such a way that adjacent cells will operate on three different sets of subcarriers, as shown in Fig. 1. We define $N_I$ and $N_O$ as the number of subcarriers allocated to the inner layer and each of the outer layers, respectively, it thus holds that $N_T = N_I + 3N_O$.

### B. Four-layer FFR network layout

In multi-layer FFR scheme deployments, a middle layer is inserted in between the inner and the outer ones. The rationale behind the use of this extra layer is to avoid excessively large inner and outer layers that lead to an overall performance degradation of the system. The reuse factor of inner layers should be small (e.g., reuse-1) to keep a relatively high spectrum utilization. In contrast, the reuse factor of outer layers should be large (e.g., reuse-3) in order to avoid high levels of ICI affecting the MSs located far from the BS. In [4], Wang *et al.* split the middle layer into two sublayers, i.e., middle1 and middle2, both implementing a reuse factor 3/2, as shown in Fig. 2. This is a feasible and practical choice for the design of a four-layer FFR scheme, and also advantageous from a performance point of view [4]. The inner and outer layers are designed in the same way as the traditional

FFR scheme. Again, for analytical tractability, the inner ($I$), middle1 ($M_1$), middle2 ($M_2$) and outer ($O$) layers will be separated by circumferences of radii $R_{th}$, $R_{M_1}$ and $R_{M_2}$.

Moreover, the set $\mathcal{F}_T$ is split into sets $\mathcal{F}_I$, $\mathcal{F}_M$ and $\mathcal{F}_O$ of subcarriers allocated to the centre, middle and outer layers, respectively. Sets $\mathcal{F}_M$ and $\mathcal{F}_O$ are further split into three equal parts, namely $\mathcal{F}_{M1}$, $\mathcal{F}_{M2}$ and $\mathcal{F}_{M3}$, which are allocated to middle-cell MSs and $\mathcal{F}_{O1}$, $\mathcal{F}_{O2}$ and $\mathcal{F}_{O3}$ which are allocated to outer-cell MSs, respectively (see Fig. 2). We have that $N_T = N_I + 3N_M + 3N_O$, where $N_M$ is the number of subcarriers allocated to each of the middle layers.

### C. Statistical characterization of the SINR

For the sake of analytical simplicity and in line with most previous studies on this topic (see, for instance, [6], [8], [11], [13], [14]), only pathloss and small scale fading are considered in this paper and hence, the channel characterizing the link between the $b$th BS and the $u$th MS can be modeled as

$$L_{\text{dB}}\left(d_{b,u}\right) = K + 10\alpha \log_{10}\left(d_{b,u}\right), \tag{2}$$

where $K$ and $\alpha$ are, respectively, the path loss at a distance of one meter from the BS and the path loss exponent, and $d_{b,u}$ is the distance (in meters) between the BS $b$ and the MS $u$.

Consider that MS $u$ is located in cell layer $A$ served by the BS of interest, where $A$ is a token used to represent any of the cell layers (or regions) $I$, $M_1$, $M_2$, or $O$. The instantaneous SINR experienced by this MS on the $n$th subcarrier and during the scheduling period $t$ can be expressed as

$$\gamma^A_{u,n}(t) = \frac{P_s G_T L(d_{0,u}) |H_{0,u,n}(t)|^2}{N_0 F_n \Delta f + I^A_{u,n}(t)}, \tag{3}$$

where $P_s$ is the power allocated per subcarrier, $G_T$ is the power gain of the BS antenna, $H_{b,u,n}(t) \sim \mathcal{CN}(0,1)$ is the frequency response resulting from the small-scale fading channel linking the $b$th BS to MS $u$ on the $n$th subcarrier during scheduling period $t$, $N_0$ is the noise power spectral density, $F_n$ is receiver noise factor and $I^A_{u,n}(t)$ denotes the interference term that is given by

$$I^A_{u,n}(t) = \sum_{b \in \Phi^A_n} P_s G_T L\left(d_{b,u}\right) |H_{b,u,n}(t)|^2, \tag{4}$$

with $\Phi^A_n$ representing the set of interfering BSs, which is subcarrier-dependent according to which layer subcarrier $n$ belongs to. In fact, assuming the BS numbering used in Figs. 1 and 2, we have that

$$\Phi^A_n = \begin{cases} \{1,2,...,18\}, & n \in \mathcal{F}_I \\ \{8,10,12,14,16,18\}, & n \in \mathcal{F}_O \end{cases}, \tag{5}$$

for the two-layer FFR scheme, and

$$\Phi^A_n = \begin{cases} \{1,2,...,18\}, & n \in \mathcal{F}_I \\ \{2,4,6,7,8,10,11,12,14,15,16,18\}, & n \in \mathcal{F}_{M_1} \\ \{1,3,5,8,9,10,12,13,14,16,17,18\}, & n \in \mathcal{F}_{M_2} \\ \{8,10,12,14,16,18\}, & n \in \mathcal{F}_O. \end{cases} \tag{6}$$

when implementing the four-layer FFR strategy. Assuming the use of uniform power allocation, the allocated power per-subcarrier can be obtained as

$$\begin{aligned} \text{Two-layer FFR: } P_s &= \frac{P_T}{N_I + N_O}, \\ \text{Four-layer FFR: } P_s &= \frac{P_T}{N_I + 2N_M + N_O}, \end{aligned} \tag{7}$$

where $P_T$ represents the available transmit power at the BS.

Note that $L\left(d_{b,u}\right)$ can be expressed in terms of the polar coordinates of MS $u$ with respect to BS 0 as $L(d_{0,u}, \theta_{0,u})$ and thus, strictly speaking, $\gamma_{u,n}(t)$ is a function of $d_{0,u}$ and $\theta_{0,u}$. Furthermore, it is shown in [20] that the instantaneous SINR in multicell networks barely depends on the polar angle and thus, from this point onwards, the dependence of $\gamma_{u,n}(t)$ on $\theta_{0,u}$ will be omitted. Moreover, since the channel is assumed to be stationary, from this point onwards the time dependence of all variables will be dropped unless otherwise stated.

Since $h_b \triangleq |H_{b,u,n}|^2$ conforms to an exponential distribution with probability density function (PDF) given by $f_{h_b}(x) = e^{-x}u(x)$, where $u(x)$ represents the unit step function, its corresponding cumulative distribution function (CDF) can be obtained as

$$F_{h_b}(x) = \Pr\{h_b \leq x\} = (1 - e^{-x})u(x). \tag{8}$$

Hence, the CDF of the instantaneous SINR $\gamma^A_{u,n}$ conditioned on the set of small-scale fading gains $\boldsymbol{h} \triangleq \{h_b\}_{\forall b \neq 0}$ and on the location of MS $u$, can be derived from (3) as

$$\begin{aligned} F_{\gamma^A_{u,n}|\boldsymbol{d},\boldsymbol{h}}(x|d,\boldsymbol{h}) &\triangleq \Pr\{\gamma^A_{u,n} \leq x|d,\boldsymbol{h}\} \\ &= \Pr\left\{ h_0 \leq \frac{\left(N_0\Delta f + I^A_{u,n}\right)}{\bar{\gamma}_0} x|d,\boldsymbol{h} \right\} \\ &= 1 - e^{-\frac{x\left(N_0\Delta f + I^A_{u,n}\right)}{\bar{\gamma}_0}}, \qquad x \geq 0, \end{aligned} \tag{9}$$

where $\bar{\gamma}_0 = P_n L(d)$ represents the average received signal. Note that distances in the set $\boldsymbol{d}$ can be written in terms of the distance $d_{0,u} = d$ from the serving BS to MS $u$.

Now, using (9) and averaging over the PDFs of the i.i.d. random variables $\boldsymbol{h}$, the conditional CDF of the instantaneous SINR $\gamma^A_{u,n}$ experienced by MS $u$ located at distance $d_{0,u} = d$ from the serving BS and in the region $A$, can be obtained as

$$\begin{aligned} &F_{\gamma^A_{u,n}|d_{0,u}}(x|d) \triangleq \Pr\{\gamma^A_{u,n} \leq x|d\} \\ &= \int_0^\infty \cdots \int_0^\infty \left(1 - e^{-\frac{x\left(N_0\Delta f + I^A_{u,n}\right)}{\bar{\gamma}_0}}\right) \prod_{i \in \Phi^A_n} f_{h_i}(h_i) \mathrm{d}h_i \\ &= 1 - e^{-\frac{xN_0\Delta f}{\bar{\gamma}_0}} \int_0^\infty \cdots \int_0^\infty e^{-\frac{x\left(\sum_{i\in\Phi^A_n} h_i \bar{\gamma}_i\right)}{\bar{\gamma}_0}} \prod_{i \in \Phi^A_n} e^{-h_i} \mathrm{d}h_i \\ &= 1 - e^{-\frac{xN_0\Delta f}{\bar{\gamma}_0}} \prod_{i \in \Phi^A_n} \frac{1}{1 + \frac{x\bar{\gamma}_i}{\bar{\gamma}_0}}, \ x \geq 0, \end{aligned} \tag{10}$$

where $f_{h_i}(h_i)$ is the PDF of the variable $h_i = |H_{i,u,n}|^2$, and $\bar{\gamma}_i = P_n L\left(d_{i,u}\right)$ is the average interfering signal from each interfering BS.

## III. Throughput analysis

The average cell throughput for the downlink of the multi-layer FFR-aided OFDMA-based cellular network can be expressed as

$$\overline{\eta} = \sum_{\forall A} \overline{\eta}^A, \tag{11}$$

where $\overline{\eta}^A$ is the average throughput of cell layer $A$.

Let us define $M_{\mathcal{S}_0}$ as a positive integer random variable representing the number of MSs in the cell served by the tagged BS. As MSs are assumed to be uniformly distributed in the entire cell region, the probability that an MS is located in cell layer $A$ is

$$P_r^A = \frac{A_r^A}{A_r^{\mathcal{H}}} = \frac{{R_U^A}^2 - {R_L^A}^2}{R^2 - R_0^2}, \tag{12}$$

where $A_r^A$ is the area of cell region $A$, and $R_L^A$ and $R_U^A$ denote the lower and upper radii of the circumferences defining this layer. Using these definitions, the average throughput in cell layer $A$ can be expressed as shown in (13) and (14) on top of the next page, for both the two-layer and the four-layer FFR schemes, respectively, where $\overline{\eta}_n^A(k_A)$ is the average throughput for the $n$th subcarrier when there are $k_A$ MSs in cell region $A$.

Now, defining $M_A$ as a non-negative integer random variable representing the number of MSs in cell region $A$, the average throughput for the $n$th subcarrier allocated to cell region $A$ when $M_A = k$, can be obtained as

$$\begin{aligned}\overline{\eta}_n^A(k) &= \Delta f \; \mathbb{E}_{\gamma_n^A|M_A}\left\{\log_2\left(1+\gamma_n^A\right)|M_A = k\right\} \\ &= \Delta f \log_2 e \int_0^\infty \frac{1 - F_{\gamma_n^A|M_A}(x|k)}{1+x}\,\mathrm{d}x.\end{aligned} \tag{15}$$

In order to obtain tractable mathematical expressions for $\overline{\eta}_n^A(k)$, the conditional CDF $F_{\gamma_n^A|M_A}(x|k)$ has to be calculated and this depends on the specific scheduling policy applied by the resource allocation algorithm. In the following subsections, this CDF will be obtained for the PF and RR scheduling rules.

### A. PF scheduling

A PF scheduler, exploiting the knowledge of the instantaneous SINRs experienced by all MSs $q \in \mathcal{M}_A$, allocates the subcarrier $n \in \mathcal{F}_A$ to MS $u \in \mathcal{M}_A$ satisfying

$$u = \arg\max_{q\in\mathcal{M}_A}\{w_q(t)\gamma_{q,n}^A(t)\}, \tag{16}$$

where $\mathcal{M}_A$ is the set indexing all MSs in cell region $A$, and $w_q(t) = 1/\mu_q(t)$ is the weighting (prioritization) coefficient for MS $q$ that, in this case, depends on the short-term average evolution of channel-state information. This can be obtained using a moving average over a window of $W$ scheduling periods as

$$\mu_q(t) = \left(1 - \frac{1}{W}\right)\mu_q(t-1) + \sum_{n\in\mathcal{F}_A} \iota_{q,n}(t)\frac{\gamma_{q,n}^A(t)}{W}, \tag{17}$$

with $\iota_{q,n}(t)$ denoting the indicator function of the event that MS $q$ is scheduled to transmit on the $n$th subcarrier during scheduling period $t$, that is,

$$\iota_{q,n}(t) = \begin{cases}1, & \text{if MS } q \text{ is scheduled on carrier } n \text{ in } t\\ 0, & \text{otherwise.}\end{cases} \tag{18}$$

From [21] we know that, for large values of $W$ and once the PF scheduler reaches stability, $\mu_q(t)$ varies very little with $t$ and thus, it can be safely approximated by its statistical expectation, that is, $\mu_q(t) \simeq \mathbb{E}\{\mu_q(t)\} \triangleq \overline{\mu}_q$. Hence, using this approximation and according to the previous definition, MS $u \in \mathcal{M}_A$ will be scheduled on subcarrier $n \in \mathcal{F}_A$ whenever

$$\varphi_{u,n}^A(t) > \varphi_{\max,u,n}^A(t) \triangleq \max_{\substack{q\in\mathcal{M}_A\\ q\neq u}}\left\{\varphi_{q,n}^A(t)\right\}, \tag{19}$$

where $\varphi_{q,n}^A(t) \triangleq \gamma_{q,n}^A(t)/\overline{\mu}_q$. That is, MS $u \in \mathcal{M}_A$ is allocated subcarrier $n$ during time slot $t$ if

$$\gamma_{u,n}^A(t) > \overline{\mu}_u \varphi_{\max,u,n}^A(t). \tag{20}$$

Thus, taking into account the fact that the random variables $\{\varphi_{q,n}^A(t)\}_{\forall\, q\in\mathcal{M}_A}$ are independent, the conditional CDF of $\gamma_n^A$, conditioned on the event that there are $M_A = k$ MSs in region $A$ and on the set of distances $\boldsymbol{d} = \{d_{0,u}\}_{\forall\, u\in\mathcal{M}_A}$, can be readily evaluated as

$$\begin{aligned}F_{\gamma_n^A|M_A,\boldsymbol{d}}(\gamma|k,\boldsymbol{d}) &= \Pr\left\{\gamma_n^A \le \gamma | M_A = k, \boldsymbol{d}\right\} \\ &= \sum_{\forall\, u\in\mathcal{M}_A} \Pr\left\{\gamma_{u,n}^A(t) \le \gamma, \varphi_{\max,u,n}^A(t) \le \frac{\gamma_{u,n}^A(t)}{\overline{\mu}_u}\,\middle|\,\boldsymbol{d}\right\} \\ &= \sum_{\forall\, u\in\mathcal{M}_A} \int_0^\gamma f_{\gamma_{u,n}^A|d_{0,u}}(x|d_{0,u}) F_{\varphi_{\max,u,n}^A|\boldsymbol{d}}\left(\frac{x}{\overline{\mu}_u}\,\middle|\,\boldsymbol{d}\right)\mathrm{d}x \\ &= \sum_{\forall\, u\in\mathcal{M}_A} \int_0^\gamma f_{\gamma_{u,n}^A|d_{0,u}}(x|d_{0,u}) \\ &\qquad \times \prod_{\substack{q\in\mathcal{M}_A\\ q\neq u}} F_{\varphi_{q,n}^A|d_{0,q}}\left(\frac{x}{\overline{\mu}_u}\,\middle|\,d_{0,q}\right)\mathrm{d}x,\end{aligned} \tag{21}$$

where $F_{\varphi_{\max,q,n}^A|\boldsymbol{d}}\left(x|\boldsymbol{d}\right)$ is the conditional CDF of $\varphi_{\max,q,n}^A(t)$ conditioned on the set of distances $\boldsymbol{d}$, and $f_{\gamma_{q,n}^A|d_{0,q}}(x|d_{0,q})$ and $F_{\varphi_{q,n}^A|d_{0,q}}(x|d_{0,q})$ are used to denote, respectively, the conditional PDF of $\gamma_{q,n}^A(t)$ and the conditional CDF of $\varphi_{q,n}^A(t)$ conditioned on $d_{0,q}$.

In order to obtain further analytical simplifications, let us assume that for each subcarrier $n$, the conditional random variables $\{\varphi_{q,n}^A|d_{0,q}\}_{\forall\, q\in\mathcal{M}_A}$ are independent and identically distributed (i.i.d.). That is, given the positions of MSs in region $A$, it is assumed that on each subcarrier $n$ in region $A$ the MSs are statistically equivalent in terms of the scheduling metrics [14]. Using this general assumption and applying integration by parts, the conditional CDF in (21) simplifies to

$$F_{\gamma_n^A|M_A,\boldsymbol{d}}(x|k,\boldsymbol{d}) = \frac{1}{k}\sum_{u\in\mathcal{M}_A} F_{\gamma_{u,n}^A|d_{0,u}}^k\left(x|d_{0,u}\right), \tag{22}$$

where $F_{\gamma_{u,n}^A|d_{0,u}}(x|d)$ is the conditional CDF of the instantaneous SINR experienced by MS $u$ on the $n$th subcarrier, which was obtained in (10).

$$\text{Two-layer FFR scheme: } \overline{\eta}^{A} = \sum_{k=1}^{\infty} \Pr\{M_{\mathcal{S}_0} = k\} \sum_{k_I=0}^{k} \binom{k}{k_I, k-k_I} \left(P_r^I\right)^{k_I} \left(P_r^O\right)^{k-k_I} \left[N_A \overline{\eta}_n^A(k_A)\right]. \tag{13}$$

$$\begin{aligned}\text{Four-layer FFR scheme: } \overline{\eta}^{A} = \sum_{k=1}^{\infty} \Pr\{M_{\mathcal{S}_0} = k\} \sum_{k_I=0}^{k} \sum_{k_{M_1}=0}^{k-k_I} \sum_{k_{M_2}=0}^{k-k_I-k_{M_1}} \binom{k}{k_I, k_{M_1}, k_{M_2}, k-k_I-k_{M_1}-k_{M_2}} \\ \times \left(P_r^I\right)^{k_I} \left(P_r^{M_1}\right)^{k_{M_1}} \left(P_r^{M_2}\right)^{k_{M_2}} \left(P_r^O\right)^{k-k_I-k_{M_1}-k_{M_2}} \left[N_A \overline{\eta}_n^A(k_A)\right].\end{aligned} \tag{14}$$

Now, taking into account the fact that on each subcarrier $n$ in region $A$, and after averaging over the distance to the BS, the MSs are statistically equivalent in terms of SINR, the (unconditional) random variables $\{\gamma_{q,n}^A(t)\}_{\forall\, q \in \mathcal{M}_A}$ are i.i.d., and the conditional CDF in (15) can be obtained as

$$F^{\text{PF}}_{\gamma_n^A|M_A}(x|k) = \int_{R_L^A}^{R_U^A} F^k_{\gamma_{u,n}^A|d_{0,u}}\left(x|d\right) f_{d_{0,u}}(d)\,\mathrm{d}d, \tag{23}$$

where $f_{d_{0,u}}(d)$ is the probability density function (PDF) of the random variable $d_{0,u}$ that can be expressed as

$$f_{d_{0,u}}(d) = \frac{2\pi d}{A_r^A},\ R_L^A \leq d \leq R_U^A. \tag{24}$$

Using (24), (23) and (15) in (13) or (14) and after some algebraic manipulations, the average throughput in cell layer $A$, for the PF scheduling rule, can be obtained as shown in (25) on top of the next page.

### *B. RR scheduling*

A RR scheduler allocates subcarriers to MSs in a fair time-sharing approach. Since the SINRs experienced by MSs in region $A$ on each subcarrier $n$ are statistically equivalent, serving $M_A = k$ MSs using a RR scheduling policy is equivalent to serving $M_A = 1$ MS with PF (even when the MSs are selected with non uniform probability). Therefore, the conditional CDF in (15) simplifies to

$$F^{\text{RR}}_{\gamma_n^A}(x) = F^{\text{PF}}_{\gamma_n^A|M_A}(x|1) = \int_{R_L^A}^{R_U^A} F_{\gamma_{u,n}^A|d_{0,u}}\left(x|d\right) f_{d_{0,u}}(d)\,\mathrm{d}d. \tag{26}$$

Finally, using (26), (24), and (15) in (13) or (14) and after some algebraic manipulations, the average throughput in the cell layer $A$, for the RR scheduling rule, can be obtained as shown in (27) on top of the next page.

### *C.* Worst *MSs' throughput: PF and RR*

Multi-layer designs and related optimization problems posed in the next section aim to maximize the throughput performance levels of the *worst* MSs in the network. Hence, it is important that the characterization of what is considered to be the throughput performance of one of the *worst* MSs in the system is clearly stated. Let us define the edge of region $A$ as a thin annular region with inner radius $R_L^{A,\text{edge}} = R_U^A - \delta$ and outer radius $R_U^{A,\text{edge}} = R_U^A$, where

$$\delta \triangleq \min\left\{\delta_0, \left(R_U^A - R_L^A\right)/2\right\}, \tag{28}$$

with $\delta_0$ denoting the maximum width of the annular region under consideration. The MSs located in this annular region experience, on average, the lowest SINRs amongst those experienced by MSs located in region $A$. Consequently, the average throughput that can be measured in this annular region represents the *worst* MSs' throughput. By a slight abuse of notation, we can substitute $R_L^A$ by $R_L^{A,\text{edge}}$ in the integration limits in (25) and (27) to obtain the average throughput $\overline{\eta}^A_{\text{edge}}$ characterizing the performance of the *worst* MSs located in region $A$ for both PF and RR scheduling rules, respectively.

## IV. Multi-layer Designs and Optimization

In this section, two fractional frequency reuse designs are explored:

- Area-proportional Design (ApD): Under this criterion, which enforces some degree of fairness among MSs, the portions of spectrum allocated to the different cell-layers are proportional to their areas.
- Free FFR Design (FrD): Under this approach, the spectrum allocation process is not tied to the spatial allocation of the different cell-layers and therefore, the design has an additional degree of freedom with respect to the ApD. This can be exploited to further increase the throughput fairness among MSs without sacrificing, and even sometimes by improving, the average cell throughput.

Furthermore, for each of these designs, a max-min optimization problem is defined for the spatial throughput experienced by the *worst* MSs in the system.

In a conventional two-layer FFR-aided scenario, the parameters typically used to pose the aforementioned problems are the distance threshold ratio $\omega \triangleq R_{th}/R$ and the spectrum allocation factor $\rho \triangleq N_I/N_T$. Appropriate selection of these parameters serves to improve the quality of experience of the *worst* users in the system, as well as the overall cell throughput. In an scenario using a four-layer FFR-aided scheme, however, new parameters are required to establish the connection between the distance thresholds used to shape the four layers and the fractions of spectrum allocated to users

$$\text{PF: } \overline{\eta}^A = \frac{2\pi N_A \Delta f \log_2 e}{A_r^A} \int_0^{\infty} \int_{R_L^A}^{R_U^A} \left(1 - \exp\left[-\pi\lambda(R^2 - R_0^2) P_r^A \left(1 - F_{\gamma_{u,n}^A | d_{0,u}}(x|d)\right)\right]\right) \frac{d}{1+x} \mathrm{d}d \ \mathrm{d}x. \tag{25}$$

$$\text{RR: } \overline{\eta}^A = \frac{2\pi N_A \Delta f \log_2 e}{A_r^A} \left(1 - \exp\left[-\pi\lambda(R^2 - R_0^2) P_r^A\right]\right) \int_0^{\infty} \int_{R_L^A}^{R_U^A} \left(1 - F_{\gamma_{u,n}^A | d_{0,u}}\left(x|d\right)\right) \frac{d}{1+x} \mathrm{d}d \ \mathrm{d}x. \tag{27}$$

located in these layers. In particular, in addition to $\omega$ and $\rho$, two new parameters can be defined as $\beta \triangleq N_M/N_O$ and $\zeta \triangleq A_r^M/A_r^O$. Even though optimizing the four-layer FFR-scheme with respect to parameters $\omega$, $\rho$, $\beta$ and $\zeta$ provides the best performance results, this is more complex when compared to the two-layer approach. In order to avoid this growth of complexity, as proposed by Wang *et al.* in [4], both $\beta$ and $\zeta$ will be set to $1/5$, which was shown to be a good choice to reach a proper tradeoff between spectral efficiency and fairness [22]. Accordingly, when using the four-layer FFR scheme, it will be assumed that

$$\frac{N_M}{N_O} = \frac{A_r^{M_1}}{A_r^O} = \frac{A_r^{M_2}}{A_r^O} = \frac{1}{5}. \tag{29}$$

Note that, from (29), the radii of the middle1 and middle2 layers can be straightforwardly expressed in terms of the distance threshold ratio $\omega$.

Before delving into details, it is worth stressing that the number of subcarriers allocated to the inner layer $N_I$ must be a non-negative integer less or equal than $N_T$. Hence, the spectrum allocation factor $\rho$ can only take values in the set

$$\mathcal{S}_\rho = \left\{ \frac{N_b - 3\lfloor N_b/3 \rfloor}{N_b}, \frac{N_b - 3(\lfloor N_b/3 \rfloor - 1)}{N_b}, \ldots, 1 \right\}, \tag{30}$$

for the two-layer FFR scheme, where $\lfloor \cdot \rfloor$ denotes the floor operator, and in the set

$$\mathcal{S}_\rho = \left\{ \frac{N_b - 18\lfloor N_b/18 \rfloor}{N_b}, \frac{N_b - 18(\lfloor N_b/18 \rfloor - 1)}{N_b}, \ldots, 1 \right\}, \tag{31}$$

for the four-layer FFR scheme.

### A. Area-proportional Design

Under the ApD, the portion of spectrum allocated to each of the cell layers is proportional to its corresponding area [8], [14]. Consequently,

$$\frac{N_I}{A_r^I} = \frac{N_O}{A_r^O} \tag{32}$$

for the two-layer FFR scheme, and

$$\frac{N_I}{A_r^I} = \frac{N_M}{A_r^{M_1}} = \frac{N_M}{A_r^{M_2}} = \frac{N_O}{A_r^O} \tag{33}$$

for the four-layer FFR system. From either (32) or (33), the spectrum allocation factor $\rho$ can be written as a function of the distance threshold ratio $\omega$. Therefore, only the parameter $\omega$ remains to be optimized. In order to maximize the spatial capacity that can be achieved by the *worst* MSs in the cell, the proposed optimization problem can then be formulated as

$$\omega^* = \arg \max_{0 \le \omega \le 1} \left( \min_{\forall A} (\overline{\eta}_{\text{edge}}^A(\omega)/A_r^A) \right). \tag{34}$$

This optimization problem guarantees the max-min fairness for cell-edge MSs under the ApD approach [4].

TABLE I: Network parameters

| System parameter | Value |
|---|---|
| Cell radius ($R$) | 500 m |
| Minimum distance from BS to MSs ($R_0$) | 35 m |
| Maximum width of a layer edge ($\delta_0$) | 4 m |
| Transmit power of the BS ($P_T$) | 46 dBm |
| Antenna gain at the BS ($G_T$) | 14 dBi |
| Noise power spectral density ($N_0$) | -174 dBm/Hz |
| Receiver noise figure ($10\log_{10} F_n$) | 7 dB |
| Total bandwidth ($B$) | 20 MHz |
| Subcarrier spacing ($\Delta f$) | 15 kHz |
| Occupied subcarriers (including DC) | 1201 |
| Path loss model | $15.3 + 37.6\log_{10}(d)$ dB |

### B. Free FFR-based Design

Under the FrD approach, both the distance threshold ratio $\omega$ and the spectrum allocation factor $\rho$ must be jointly optimized. Hence, the proposed optimization problem can be particularized to this approach as

$$(\omega^*, \rho^*) = \arg \max_{\substack{0 \le \omega \le 1 \\ \rho \in \mathcal{S}_\rho}} \left( \min_{\forall A} \frac{\overline{\eta}_{\text{edge}}^A(\omega, \rho)}{A_r^A} \right). \tag{35}$$

This problem can be easily solved in two steps. In the first step, the FFR spectrum allocation factor is fixed to $\rho = \rho_0$ and an optimization subproblem equivalent to (35) is posed for each individual $\rho_0$ value in the set $\mathcal{S}_\rho$. That is,

$$\omega^\dagger(\rho_0) = \arg \max_{0 \le \omega \le 1} \left( \min_{\forall A} \frac{\overline{\eta}_{\text{edge}}^A(\omega, \rho_0)}{A_r^A} \right), \tag{36}$$

where the superscript $(\cdot)^\dagger$ is used to indicate the optimal solutions to these subproblems. Once we have obtained the distance threshold ratios $\omega^\dagger(\rho_0)$ for all $\rho_0 \in \mathcal{S}_\rho$, the optimal FFR-related parameters can be obtained as $\omega^* = \omega^\dagger(\rho^*)$ with

$$\rho^* = \arg \max_{\rho_0 \in \mathcal{S}_\rho} \left( \min_{\forall A} \frac{\overline{\eta}_{\text{edge}}^A(\omega^\dagger(\rho_0), \rho_0)}{A_r^A} \right). \tag{37}$$

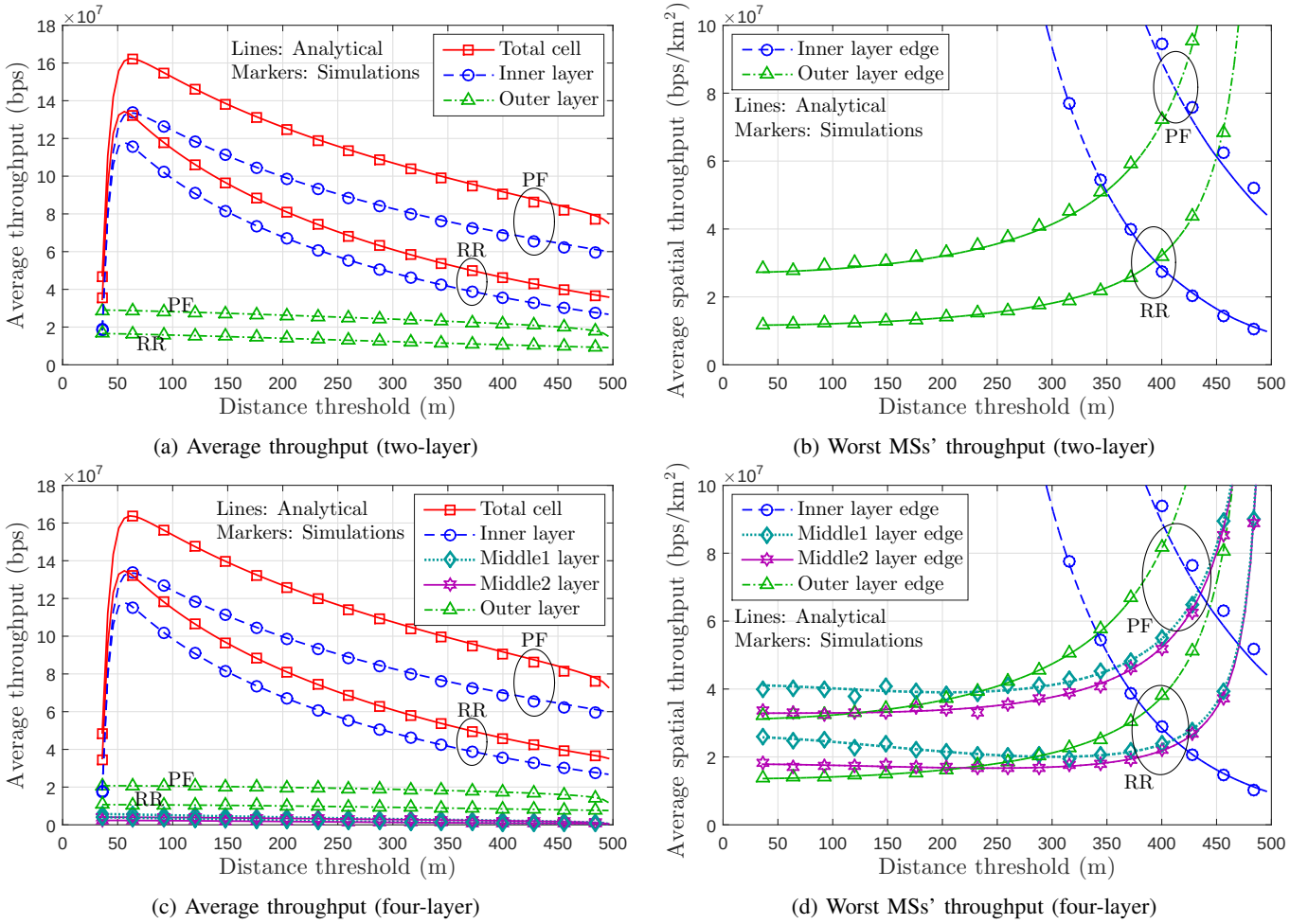


(a) Average throughput (two-layer)

(b) Worst MSs' throughput (two-layer)

(c) Average throughput (four-layer)

(d) Worst MSs' throughput (four-layer)

Fig. 3: Average layers' throughput and worst MSs' throughput as functions of the distance threshold $R_{th}$ ($M = 512$, $N_I = 624$ and $N_M = 32$).

## V. Performance Evaluation

The performance evaluation scenario under consideration is a 19-cell network where the cell of interest is surrounded by two rings of interfering BSs (see Figs. 1 and 2). As stated in previous sections, MSs are distributed over the coverage area using a PPP of normalized intensity $\lambda$ (measured in MSs per unit area) but, for the sake of presentation clarity, results in this section will be shown as a function of the average number of MSs per cell ($M \triangleq \pi\lambda(R^2 - R_0^2)$). The main system parameters used to generate both the analytical and simulation results are based on [23] and summarized in Table I.

In order to validate the proposed analytical framework, results in Fig. 3 show the average cell throughput, the per-layer average throughput and the average throughput allocated to the *worst* MSs in each layer. Results are given for the two-layer and the four-layer FFR schemes, and using either PF or RR scheduling policies. These results have been obtained for an average number of MSs per cell $M = 512$ and a fixed spectrum allocation factor $\rho = 0.52$. Note that lines are used to represent the analytical results and markers correspond to results obtained through Monte-Carlo simulations. A very good agreement between the simulation and analytical results can be observed, thus validating the novel theoretical framework presented in Section III.

The two metrics under study exhibit a different qualitative behaviour that is subsequently investigated. Focusing first on the average throughput depicted in Figs. 3a and 3c, it can be observed that the throughput of the middle and outer layers in the four-layer scheme, and the outer layer in the two-layer scheme, diminishes as the distance threshold increases. Also, the average throughput of the inner layer increases with the distance threshold up to a maximum (located around a distance threshold of 60 m) and then exhibits an steady decrease with the value of $\omega$. Note that these results suggest that, if average cell throughput was the only target metric, the best strategy would consist of setting the distance thresholds to a common low value of, approximately, 60 m. Optimizing only the average cell throughput would lead to a loss in fairness among the users located in different layers. For the average throughput experienced by the worst users in each of the layers (see Figs. 3b and 3d), it is worth pointing out that when the distance threshold approaches 60 m, and whatever the number of layers used in the FFR scheme, the worst users of the inner layer enjoy a much higher average throughput than the worst users in other layers.

In light of these first results, it is quite obvious that the threshold distances that maximize the average cell throughput should be avoided when the objective is to guarantee a high degree of throughput fairness among users. Instead, another optimization metric is required so as to ensure that the throughput experienced by the different users in the system is far more uniform. In particular, the selected criterion inducing the desired degree of fairness among users is a max-min metric targeting the worst users in each layer. As can be seen in Figs. 3b and 3d, the distance threshold that guarantees the optimization of this max-min criterion has to be fixed around 400 m when using an RR scheduler and to around 415 m when relying on a PF scheduler. A noteworthy fact to be appreciated in Figs. 3b and 3d is that the *worst* users in the system can be found in different layers depending on the distance threshold. For small distance thresholds the *worst* users are located in the outer layers, while for large distance thresholds they are to be found in the inner layers.

In any case, note that from this fixed spectrum allocation setup it is not possible to draw any conclusion regarding the benefit of the four-layer scheme over the two-layer one. As it will be shown next, some more elaborate designs are necessary to determine which is the best resource allocation strategy in each of the considered scenarios.

### A. ApD for a fixed value of $M$

As already mentioned, when relying on an ApD, frequency resources are distributed among the different system layers proportionally to their areas, thus making the distance threshold the only parameter to be optimized. Fig. 4 depicts the average (overall) cell throughput and the throughput of the worst users in each layer, as a function of the distance threshold for the specific case of $M = 512$ and assuming the use of PF scheduling (similar qualitative outcomes were observed for the RR case). Again, a very good agreement can be observed between analytical results (lines) and simulations (markers), validating the theoretical framework in Section IV.

One of the peculiarities of the ApD scheme is that it allocates a larger number of resources to the inner layer as the distance threshold increases. Given that the inner layers implement a reuse factor equal to 1 while the other layers implement higher reuse factors, the distance threshold affects the cell throughput. As shown in Figs. 4a and 4b, increasing the distance threshold reduces the average throughput of the outer layer in the two-layer setup and that of the middle and outer layers in the four-layer setup, while the inner layer achieves a large increase in average throughput. In fact, if average overall throughput was the only target metric, the inner layer would expand up to the cell limit conforming to a conventional cellular system with universal frequency reuse (i.e., FFR would not be used). Notice that this would imply that users located near the cell edges would suffer from much larger levels of ICI than those located near the cell centers, thus exacerbating the unfairness of this design.

Figures 4c and 4d show the results corresponding to the max-min criterion that, as previously mentioned, allows the consideration of fairness among users when optimizing the network. As can be observed in these figures, and focusing first on the two-layer FFR scheme, the operational point guaranteeing max-min fairness is located at $\omega^* = 0.486$, which is the intersection point between the curves corresponding to the worst users of the inner and outer layers. At this specific point, the max-min average spatial throughput is seen to be 66.4 Mbps/km$^2$ and the average cell throughput is equal to 64.4 Mbps. When considering the four-layer design, the optimum max-min fairness operational point is located at $\omega^* = 0.239$, corresponding to the crossing spot of the worst users in the middle2 and outer layers, and attaining an average spatial throughput of 67.3 Mbps/km$^2$ and an average cell throughput of 65.8 Mbps. When compared to the traditional two-layer design, it can be concluded that the proposed four-layer design is able to improve the max-min throughput fairness without compromising (in fact, even slightly improving) the average cell throughput.

### B. FrD for a fixed value of $M$

The FrD-based optimization is more involved than an ApD-based one, but a superior performance is expected both in terms of max-min average spatial throughput and average cell throughput. This is because the optimization simultaneously tackles two parameters, namely, the spectrum allocation factor $\rho$ and the distance threshold $\omega$. For the sake of clarity, results are presented using bidimensional plots in Figs. 5 and 6 whereby results are shown as a function of $\omega$ and $\rho$, respectively. It should be noted that results in Fig. 5 have been obtained using $\rho^*$ and results in Fig. 6 have been obtained using $\omega^*$. In other words, the graphs shown in Fig. 5 correspond to $\overline{\eta}(\omega, \rho^*)$ and $\frac{\overline{\eta}^A_{\text{edge}}(\omega,\rho^*)}{A^A_r}$, while the graphs shown in Fig. 6 correspond to $\overline{\eta}(\omega^*, \rho)$ and $\frac{\overline{\eta}^A_{\text{edge}}(\omega^*,\rho)}{A^A_r}$. In particular, results presented in these figures show the average overall cell throughput and the average throughput for the worst users in each layer for the case of $M = 512$ and when using PF scheduling (as before, RR results do not provide any further qualitative insight).

Due to the increased number of degrees of freedom this design brings, FrD-based results are markedly different from the ones obtained when using ApD. As it can be observed in Figs 5a and 5b, assuming the use of $\rho^*$, the average throughput of the outer layer in the two-layer design and of the outer, middle1 and middel2 layers in the four-layer design, diminish with an increasing distance threshold. However, the average cell throughput of the inner layer does not steadily grow with an increasing value of $\omega$ as in the ApD approach but instead, it reaches a maximum value beyond which it begins to reduce. Summing the average throughput for all layers, and irrespective of the design being two- or four-layered, maximization of the average throughput is achieved for $\omega \simeq 0.12$. However, observe that when assessing the average spatial throughput for $\omega \simeq 0.12$ (see Figs. 5c and 5d), the worst users of the inner layer clearly outperform the worst users of the other layer in the FFR scheme, thus compromising the throughput fairness among users. Moreover, assuming the use of $\omega^*$, it can be observed in Figs. 6a and 6b that, as expected, increasing the value of the spectrum allocation factor $\rho$ results in a steady increase (decrease) of the

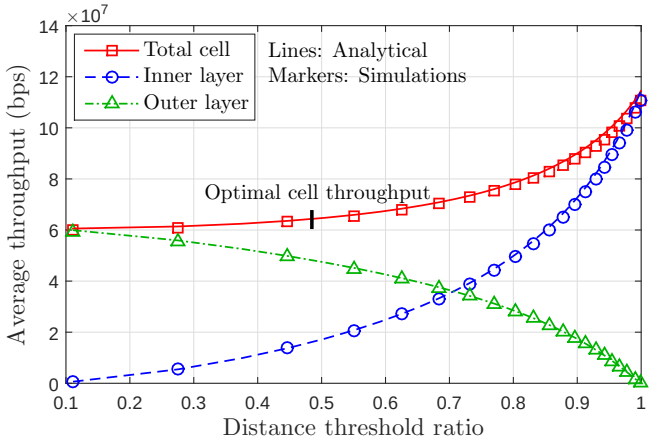


(a) Average cell throughput (two-layer)

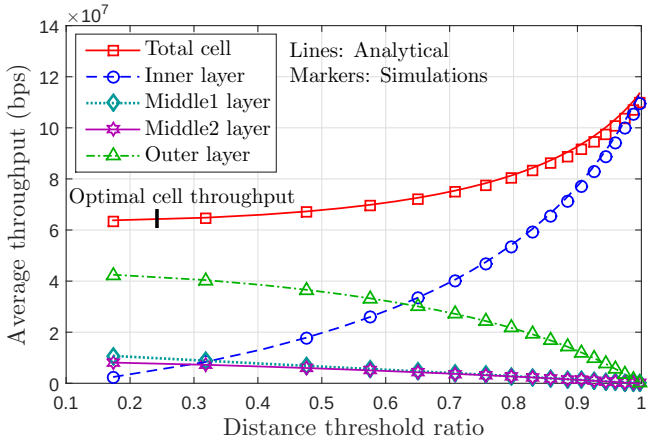


(b) Average cell throughput (four-layer)

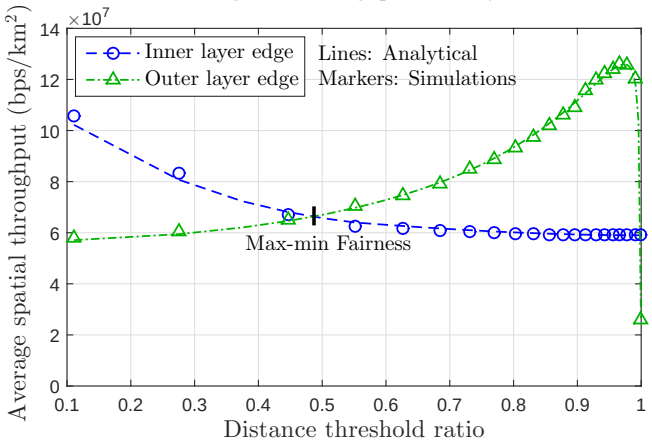


(c) Worst MSs' throughput (two-layer)

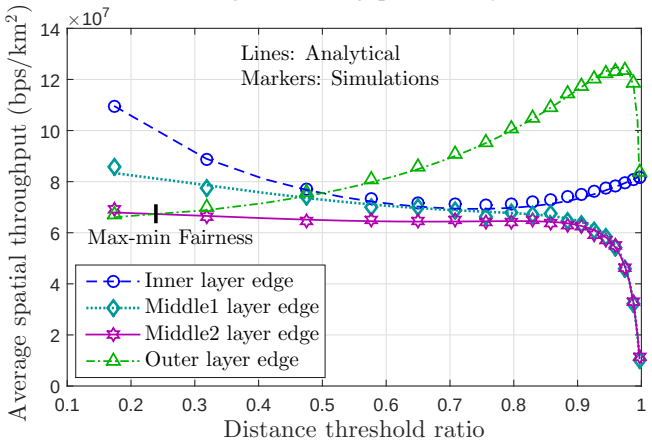


(d) Worst MSs' throughput (four-layer)

Fig. 4: Average cell throughput and average spatial throughput *versus* the distance threshold ratio $\omega$ for ApD, PF scheduler and $M = 512$.

average throughput of the inner layer (remaining layers). This is because it is (they are) allocated a larger (lower) number of spectral resources. Again, the use of $\rho = 1$ would result in the maximization of the average cell throughput but at the cost of sacrificing throughput fairness among users located at different distances from the BS.

When assessing the max-min criterion among the worst users in the different layers of the system, the optimal operating point for the two-layer FFR scheme (intersection of the worst-user average throughput for the inner and outer layers) can be seen to be located around $\omega^* = 0.396$ and $\rho^* = 0.05$, which leads to a max-min average spatial throughput of 63.2 Mbps/km$^2$ and average cell throughput of 79.1 Mbps. In the four-layer design, the max-min optimum operational point is seen to be located at $\omega = 0.355$ and $\rho^* = 0.04$ and results in an average spatial throughput of 67.0 Mbps/km$^2$ and an average cell throughput of 80.8 Mbps. Notice the improvement achieved by the four-layer design in terms of max-min performance without compromising the average cell throughput. As a final word on this design, note the very significant improvements FrD brings along in comparison to ApD.

### C. *Effects of the number of users per cell*

Concluding this numerical results section, it is interesting to study the impact network load (number of users per cell) has on the performance. To this end, plots in Fig. 7 show the optimal cell throughput and max-min fairness throughput as a function of the average number of users per cell for both ApD and FrD, and when considering two- and four-layer designs. Results for both the PF and RR scheduling rules are presented in this case. Regardless of the user density, it is very noticeable the quantitative performance advantage PF gains over RR. Another fact worth stressing is that FrD always outperforms ApD, no matter how many users are active in the system. Finally, observe how for a high user density (beyond 50 users/cell) and irrespective of the FFR design in use (either ApD or FrD), the four-layer scheme yields better max-min fairness throughput in comparison to the two-layer scheme without sacrificing the average cell throughput. It is nonetheless interesting to note a fact that went undetected in the seminal work of Wang *et. al* [4], namely, that for very low user densities, a classical two-layer FFR scheme outperforms multi-layer setups. This behavior is caused by the fact that at low user densities, there exists a non-negligible probability that some of the FFR layers are empty. This wastes the frequency

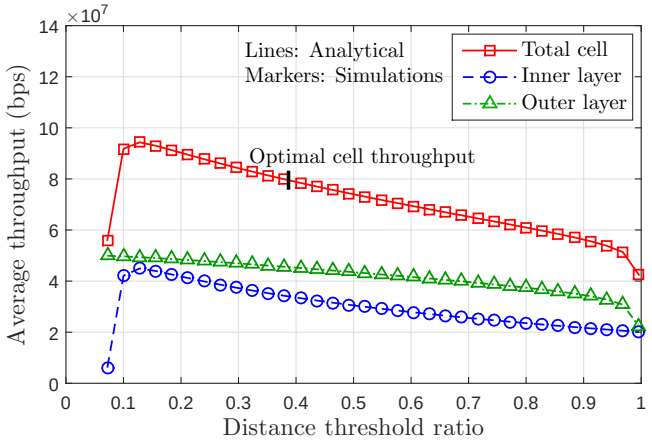


(a) Average throughput (two-layer)

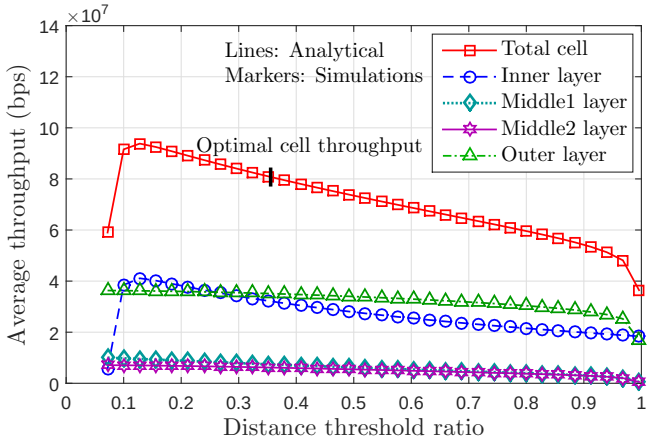


(b) Average throughput (four-layer)

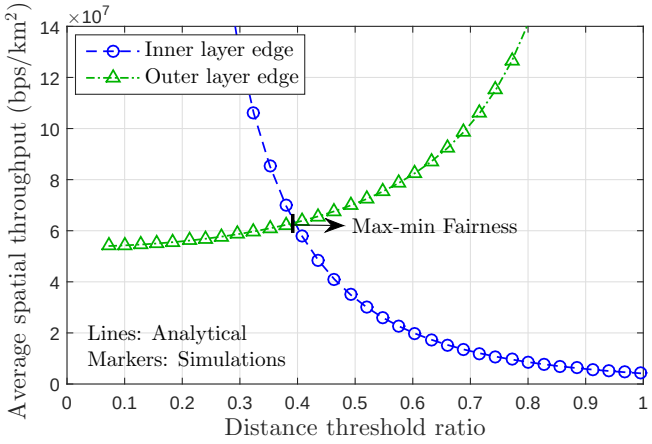


(c) Worst MSs' throughput (two-layer)

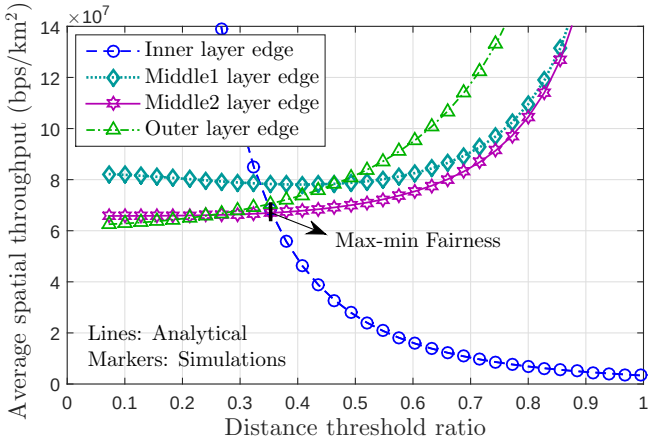


(d) Worst MSs' throughput (four-layer)

Fig. 5: Average cell throughput and average spatial throughput *versus* the distance threshold ratio $\omega$ for FrD, a PF scheduler and $M = 512$, assuming the use of $\rho^*$.

resources allocated to those layers in those particular cells. This effect opens the door to the study of adaptive FFR designs that, depending on the number of active users in the system and according to the particular optimization function the network operators pursue, determine the optimum number of FFR layers to be used.

## VI. Conclusion

This paper has presented and validated a novel analytical framework allowing the performance evaluation of multi-layer FFR-aided OFDMA-based multi-cellular networks using channel-aware schedulers. Using this theoretical framework, two multi-layer FFR-based optimal designs, termed as the area-proportional design (ApD) and the free FFR design (FrD), have been proposed to determine the appropriate size of the FFR-related spatial and spectral partitions. Moreover, for both ApD and FrD approaches, a max-min optimization problem has been defined for the *worst* users in the system. Under high user loads and irrespective of the scheduling rule in use (either PF or RR), the multi-layer FFR scheme outperforms the conventional two-layer one in terms of max-min throughput performance without compromising the average cell throughput. For very low user densities, however, a classical two-layer FFR scheme can outperform the multi-layer setups. This opens the door to adaptive multi-layer FFR designs that determine the optimum number of FFR layers to be deployed as the number of active users in the system changes. Finally, the FrD scheme provides important performance improvements when compared to the simpler ApD strategy. Further work will focus on extending the proposed analytical framework to more sophisticated ICIC techniques including soft/adaptive frequency reuse schemes, the use of higher order sectorization or the implementation of cooperative network MIMO.

## Acknowledgment

This work has been supported in part by the Agencia Estatal de Investigación and Fondo Europeo de Desarrollo Regional (AEI/FEDER, UE) under project ELISA (subproject TEC2014-59255-C3-2-R), Ministerio de Economía y Competitividad (MINECO), Spain, and the Conselleria d'Educació, Cultura i Universitats (Govern de les Illes Balears) under grant FPI/1538/2013 (co-financed by the European Social Fund). The research leading to these results has also received funding from "la Caixa" Banking Foundation.

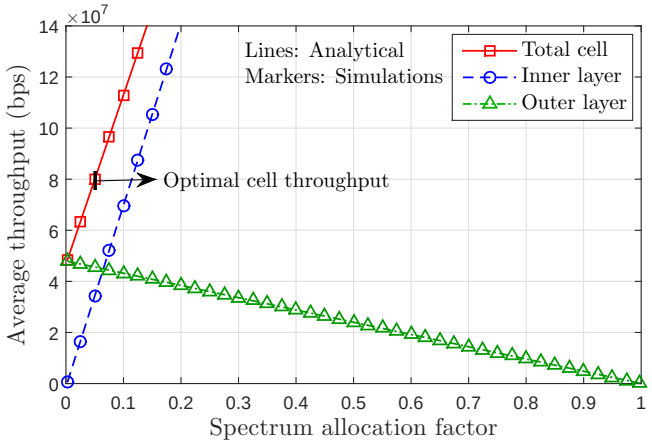


(a) Average throughput (two-layer)

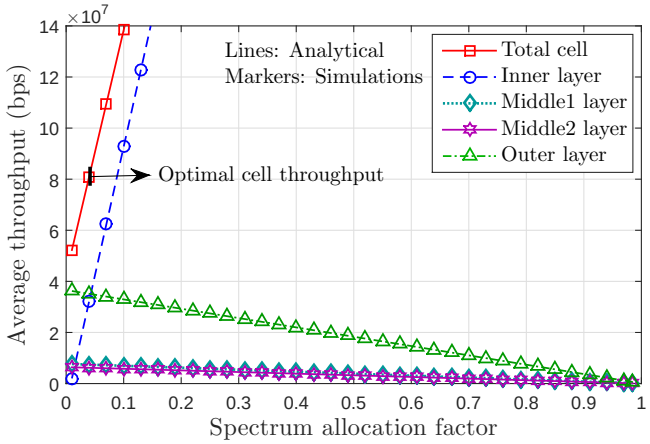


(b) Average throughput (four-layer)

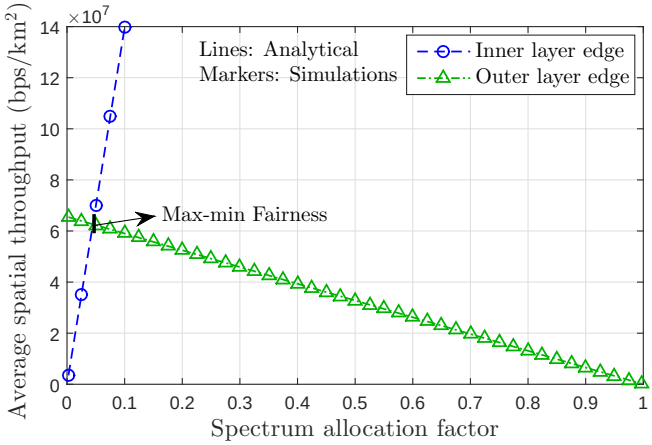


(c) Worst MSs' throughput (two-layer)

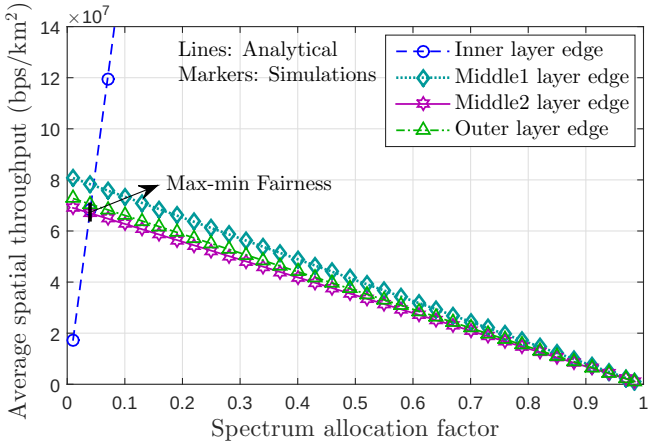


(d) Worst MSs' throughput (four-layer)

Fig. 6: Average cell throughput and average spatial throughput *versus* the spectrum allocation factor $\rho$ for FrD, a PF scheduler and $M = 512$, assuming the use of $\omega^*$.

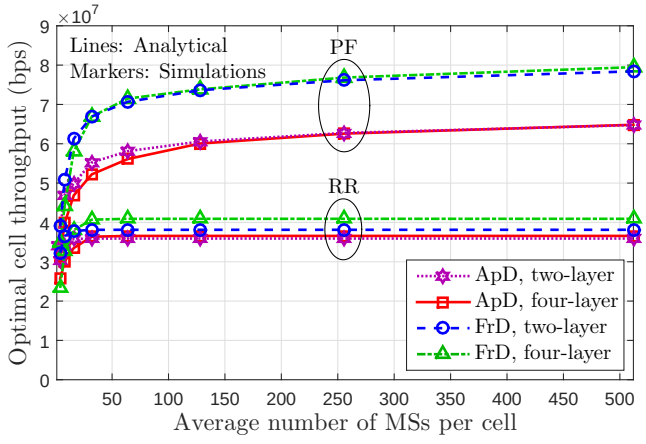


(a) Optimal average cell throughput

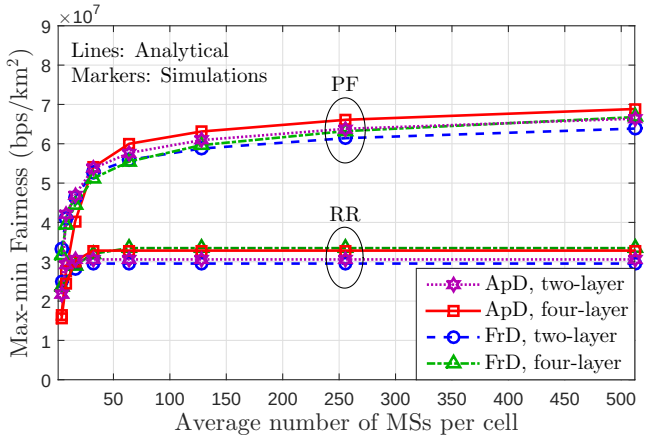


(b) Max/min fairness spatial throughput

Fig. 7: Optimal average cell throughput and max/min fairness average spatial throughput as a function of the average number of MSs per cell $M$.

## REFERENCES


[1] E. Dahlman, S. Parkvall, and J. Skold, *4G: LTE/LTE-Advanced for Mobile Broadband*, 2nd ed. Elsevier Science, 2013.

[2] A. S. Hamza, S. S. Khalifa, H. S. Hamza, and K. Elsayed, "A survey on inter-cell interference coordination techniques in OFDMA-based cellular networks," *IEEE Communications Surveys & Tutorials*, vol. 15, no. 4, pp. 1642–1670, 2013.

[3] N. Saquib, E. Hossain, and D. I. Kim, "Fractional frequency reuse for interference management in LTE-Advanced HetNets," *IEEE Wireless Communications*, vol. 20, no. 2, pp. 113–122, 2013.

[4] L. Wang, F. Fang, N. Nikaein, and L. Cottatellucci, "An analytical framework for multilayer partial frequency reuse scheme design in mobile communication systems," *IEEE Transactions on Vehicular Technology*, vol. 65, no. 9, pp. 7593–7605, 2016.

[5] F. Kelly, A. Maulloo, and D. Tan, "Rate control for communication networks: shadow prices, proportional fairness and stability," *The Journal of the Operational Research Society*, vol. 49, no. 3, pp. 237–252, 1998.

[6] T. Novlan, R. Ganti, A. Ghosh, and J. Andrews, "Analytical evaluation of fractional frequency reuse for OFDMA cellular networks," *IEEE Transactions on Wireless Communications*, vol. 10, no. 12, pp. 4294–4305, December 2011.

[7] H. ElSawy, E. Hossain, and M. Haenggi, "Stochastic geometry for modeling, analysis, and design of multi-tier and cognitive cellular wireless networks: A survey," *IEEE Communications Surveys & Tutorials*, vol. 15, no. 3, pp. 996–1019, 2013.

[8] F. Jin, R. Zhang, and L. Hanzo, "Fractional frequency reuse aided twin-layer femtocell networks: Analysis, design and optimization," *IEEE Transactions on Communications*, vol. 61, no. 5, pp. 2074–2085, 2013.

[9] M. Assaad, "Optimal fractional frequency reuse (FFR) in multicellular OFDMA system," in *IEEE 68th Vehicular Technology Conference (VTC-Fall)*, 2008, pp. 1–5.

[10] A. Najjar, N. Hamdi, and A. Bouallegue, "Efficient frequency reuse scheme for multi-cell OFDMA systems," in *IEEE Symposium on Computers and Communications (ISCC)*, 2009, pp. 261–265.

[11] Z. Xu, G. Y. Li, C. Yang, and X. Zhu, "Throughput and optimal threshold for FFR schemes in OFDMA cellular networks," *IEEE Transactions on Wireless Communications*, vol. 11, no. 8, pp. 2776–2785, 2012.

[12] G. Femenias and F. Riera-Palou, "Corrections to, and comments on, "Throughput and Optimal Threshold for FFR Schemes in OFDMA Cellular Networks"," *IEEE Transactions on Wireless Communications*, vol. 14, no. 5, pp. 2926 – 2928, 2015.

[13] J. García-Morales, G. Femenias, and F. Riera-Palou, "Analysis and optimization of ffr-aided ofdma-based heterogeneous cellular networks," *IEEE Access*, vol. 4, pp. 5111–5127, 2016.

[14] ——, "Performance analysis and optimisation of FFR-aided OFDMA networks using channel-aware scheduling," *Mobile Networks and Applications*, pp. 1–15, May 2016.

[15] H.-B. Chang and I. Rubin, "Optimal downlink and uplink fractional frequency reuse in cellular wireless networks," *IEEE Transactions on Vehicular Technology*, vol. 65, no. 4, pp. 2295–2308, 2016.

[16] S. E. Sagkriotis and A. D. Panagopoulos, "Optimal FFR policies: Maximization of traffic capacity and minimization of base station's power consumption," *IEEE Wireless Communications Letters*, vol. 5, no. 1, pp. 40–43, 2016.

[17] Z. Xie and B. Walke, "Performance analysis of reuse partitioning techniques in OFDMA based cellular radio networks," in *Telecommunications (ICT), 2010 IEEE 17th International Conference on*. IEEE, 2010, pp. 272–279.

[18] R. Ghaffar and R. Knopp, "Fractional frequency reuse and interference suppression for OFDMA networks," in *Modeling and Optimization in Mobile, Ad Hoc and Wireless Networks (WiOpt), 2010 Proceedings of the 8th International Symposium on*. IEEE, 2010, pp. 273–277.

[19] X. Yang, "A multilevel soft frequency reuse technique for wireless communication systems," *IEEE Communications Letters*, vol. 18, no. 11, pp. 1983–1986, 2014.

[20] M. Maqbool, P. Godlewski, M. Coupechoux, and J.-M. Kélif, "Analytical performance evaluation of various frequency reuse and scheduling schemes in cellular OFDMA networks," *Performance Evaluation*, vol. 67, no. 4, pp. 318–337, 2010.

[21] E. Liu and K. Leung, "Expected throughput of the proportional fair scheduling over Rayleigh fading channels," *IEEE Communications Letters*, vol. 14, no. 6, pp. 515–517, June 2010.

[22] L. Wang, F. Fang, K. Min, N. Nikaein, and L. Cottatellucci, "Toward multi-layer partial frequency reuse in future mobile communication systems," in *Communications in China (ICCC), 2014 IEEE/CIC International Conference on*. IEEE, 2014, pp. 647–652.

[23] G. TR36.921, "Home enode b (HeNB) radio frequency (RF) requirements analysis (release 9)," v9.0.0. Mar. 2010.